Dual allosteric and orthosteric pharmacology of synthetic analog cannabidiol-dimethylheptyl, but not cannabidiol, on the cannabinoid CB2 receptor

Bouma; J.; Broekhuis, J.D.; Horst, C. van der; Kumar, P.; Ligresti, A.; ... ; Heitman, L.H.

Dual allosteric and orthosteric pharmacology of synthetic analog cannabidiol-dimethylheptyl, but not cannabidiol, on the cannabinoid CB$_2$ receptor

Jara Bouma [a], Jeremy D. Broekhuis [a], Cas van der Horst [a], Poulami Kumar [b], Alessia Ligresti [b], Mario van der Stelt [c], Laura H. Heitman [a,*]

[a] *Division of Drug Discovery and Safety, LACDR, Leiden University & Oncode Institute, the Netherlands*
[b] *National Research Council of Italy, Institute of Biomolecular Chemistry, Italy*
[c] *Department of Molecular Physiology, LIC, Leiden University & Oncode Institute, the Netherlands*

ARTICLE INFO

ABSTRACT

Cannabinoid CB$_2$ receptor (CB$_2$R) is a class A G protein-coupled receptor (GPCR) involved in a broad spectrum of physiological processes and pathological conditions. For that reason, targeting CB$_2$R might provide therapeutic opportunities in neurodegenerative disorders, neuropathic pain, inflammatory diseases, and cancer. The main components from *Cannabis sativa*, such as Δ^9-tetrahydrocannabinol (Δ^9-THC) and cannabidiol (CBD), have been therapeutically exploited and synthetically-derived analogs have been generated. One example is cannabidiol-dimethylheptyl (CBD-DMH), which exhibits anti-inflammatory effects. Nevertheless, its pharmacological mechanism of action is not yet fully understood and is hypothesized for multiple targets, including CB$_2$R. The aim of this study was to further investigate the molecular pharmacology of CBD-DMH on CB$_2$R while CBD was taken along as control. These compounds were screened in equilibrium and kinetic radioligand binding studies and various functional assays, including G protein activation, inhibition of cAMP production and ß-arrestin-2 recruitment. In dissociation studies, CBD-DMH allosterically modulated the radioligand binding. Furthermore, CBD-DMH negatively modulated the G protein activation of reference agonists CP55,940, AEA and 2-AG, but not the agonist-induced ß-arrestin-2 recruitment. Nevertheless, CBD-DMH also displayed competitive binding to CB$_2$R and partial agonism on G protein activation, inhibition of cAMP production and ß-arrestin-2 recruitment. CBD did not exhibit such allosteric behavior and only very weakly bound CB$_2$R without activation. This study shows a dual binding mode of CBD-DMH, but not CBD, to CB$_2$R with the suggestion of two different binding sites. Altogether, it encourages further research into this dual mechanism which might provide a new class of molecules targeting CB$_2$R.

1. Introduction

The cannabinoid CB$_1$ and CB$_2$ receptors (CB$_1$R and CB$_2$R) are class A G protein-coupled receptors (GPCRs) that are responsible for signal transduction of the endocannabinoid system (ECS) [1]. Both receptors couple primarily to G$\alpha_{i/o}$ proteins and recruit ß-arrestin upon stimulation by agonists, such as the endocannabinoids anandamide (AEA) and 2-arachidonoylglycerol (2-AG) [2,3]. However, due to the distinct localization of these receptors, they regulate different processes. CB$_1$R is the most abundant GPCR in the central nervous system and involved in the regulation of cognition and memory. On the contrary, CB$_2$R is primarily expressed on cells of the immune system and modulates (neuro) inflammatory processes [4]. Therefore, specific targeting of CB$_2$R might provide opportunities in the treatment of a variety of pathological conditions characterized by low-grade inflammation, such as neuropathic pain, inflammatory bowel disease, neurodegenerative disorders,

and cancer [5].

The main components of *Cannabis sativa* Δ^9-tetrahydrocannabinol (Δ^9-THC) and cannabidiol (CBD), and synthetically-derived analogs have been therapeutically exploited to target CB_2R [6]. Over the years, CBD has received increasing attention due to its variety of therapeutic effects, including antiepileptic, anti-inflammatory, analgesic, and anti-cancer properties as well as neuroprotective and neuromodulatory functions in Parkinson's disease [7,8]. Currently, Epidiolex® (CBD) and Sativex® (1:1 CBD: Δ^9-THC) are approved for the treatment of Dravet syndrome, Lennox-Gastaut syndrome and multiple sclerosis-associated spasticity [9]. Additionally, CBD has been brought to the attention of the public as component of oils or infused beverages that can be obtained without a prescription [10]. However, the pharmacological mechanism of action of CBD is not yet fully understood and has been linked to interactions with various targets via contradicting mechanisms [8,11–13].

In view of the promising therapeutic possibilities of CBD, various derivatives have been synthesized over the years. One such derivative is cannabidiol-dimethylheptyl (CBD-DMH) in which the pentyl side chain of CBD is replaced for a dimethylheptyl chain (Fig. 1) [14]. Similar to CBD, CBD-DMH is devoid of any psychotropic activity and has been shown to possess anti-inflammatory effects by reducing the levels of various pro-inflammatory genes and key inflammatory mediators, such as nitric oxide and reactive oxygen intermediates [14–17]. Additionally, CBD-DMH induced apoptosis in myeloblastic cells, but not healthy control cells [18]. Fride *et al.* further demonstrated efficacy and anti-inflammatory activity of CBD-DMH *in vivo* [19]. These beneficial effects of CBD-DMH have been hypothesized to be mediated via various proteins, such as CB_2R, CB_1R, adenosine A_{2A} receptor and an anandamide transporter. [15–17,19–22]. Interestingly, low (orthosteric)
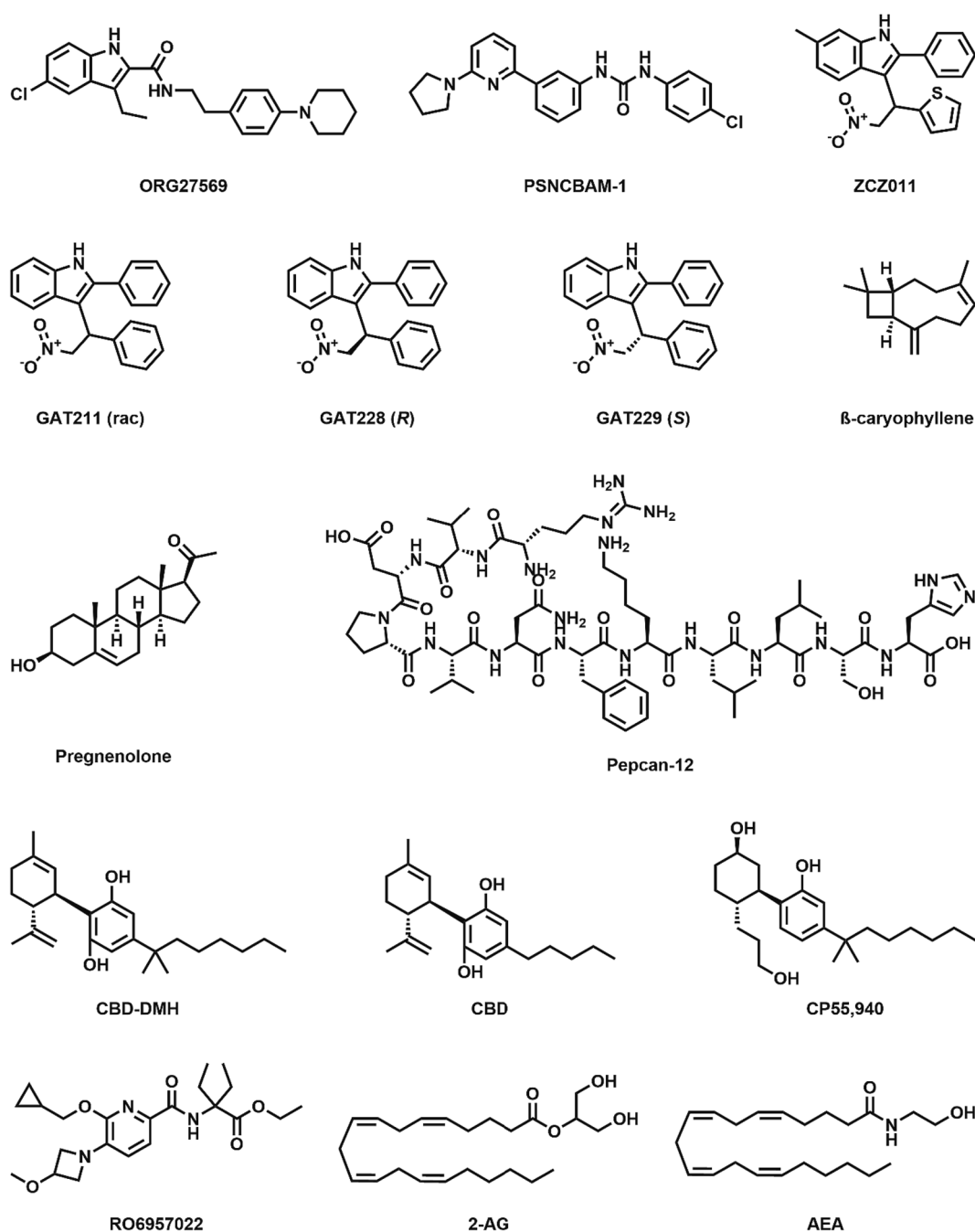

Fig. 1. Chemical structures of reported allosteric modulators and reference ligands of the endocannabinoid system.

affinity of CBD-DMH to CB_2R has been found, but also allosteric modulation of downstream signaling pathways has been speculated [20–22]. Nevertheless, the exact molecular mechanisms remain unknown.

In view of the therapeutic possibilities, we aimed to investigate the molecular pharmacological effect of CBD-DMH on CB_2R, while close analog CBD was taken along. The possibility of an allosteric interaction with CB_2R was explored in equilibrium and kinetic radioligand binding studies in which all commercially available proclaimed allosteric modulators of the ECS were screened for validation (Fig. 1) [23]. Of these, only CBD-DMH displayed allosteric properties on CB_2R and was further characterized in radioligand binding assays and functional studies. CBD-DMH demonstrated competitive binding to CB_2R and (partial) agonism on G protein activation, inhibition of cAMP production and ß-arrestin-2 recruitment. Additionally, CBD-DMH negatively impacted the affinity of a set of reference ligands. Furthermore, in the presence of CBD-DMH the G protein activation of CP55,940 and 2-AG was impaired, which was not observed in ß-arrestin-2 recruitment assays to CB_2R. This study shows that CBD-DMH has allosteric interactions with CB_2R, but also competitively binds to the receptor with orthosteric ligands. It therefore invites further research into this dual mechanism of CBD-DMH to CB_2R which might provide a new class of molecules targeting CB_2R.

2. Materials and methods

2.1. Chemicals and reagents

Compounds AM630, CP55,940, GAT228, GAT229, GAT211, pregnenolone and PSNCBAM-1 were obtained from Sigma-Aldrich (St. Louis, MO, USA). Pepcan-12 (RVD-HPα), (-)-cannabidiol (CBD), anandamide (AEA), 2-arachidonoylglycerol (2-AG) and phenylmethylsulfonyl fluoride (PMSF) were bought from Tocris Bioscience (Bristol, United Kingdom). ZCZ011 was received from Axon Medchem (Groningen, the Netherlands), while ß-caryophyllene was obtained from Bio-Connect (Huissen, the Netherlands), and (-)-5′-cannabidiol-dimethylheptyl (CBD-DMH) was from Bio-Techne Ltd (Abingdon, United Kingdom). RO6957022 and [3H]RO6957022 (specific activity 82.8 Ci/mmol) were custom-synthesized and custom-labeled, respectively, by F. Hoffmann-La Roche Ltd (Basel, Switzerland). [3H]CP55,940 (specific activity 108.5 Ci/mmol), guanosine 5′-O-[γ-thio]triphosphate ([35S]GTPγS, specific activity 1250 Ci/mmol) and GF/C filter plates were purchased from PerkinElmer (Waltham, MA, USA). The PathHunter and cAMP Hunter detection kits were obtained from DiscoverX (Fremont, CA, USA). Bicinchoninic acid (BCA) and BCA protein assay reagent were purchased from Pierce Chemical Company (Rockford, IL, USA). All other chemicals were of analytical grade and obtained from standard commercial sources. Buffers and solutions were prepared at room temperature (rt) using Millipore water (deionized using a MilliQ A10 Biocel™, with a 0.22 μm filter).

2.2. Cell culture

CHO cells stably expressing hCB_2R (CHOK1_hCB_2bgal, DiscoverX) were cultured in Ham's F12 Nutrient Mixture supplemented with 10% (v/v) fetal calf serum (FCS), 2 mM Glutamax, 100 IU/mL penicillin, 100 μg/mL streptomycin, 300 μg/mL hygromycin and 800 μg/mL G418 in a humidified atmosphere at 37 °C and 5% CO_2. Cells were subcultured twice-weekly when reaching 80–90% confluence on 10 or 15 cm ø plates by trypsinization. All experiments were done within 20 passages.

2.3. Membrane preparation

CHOK1_hCB_2bgal cells were harvested when reaching 90% confluence in 15 cm ø plates after one week subculture at a 1:6 ratio. The cells were detached by scraping into 5 mL phosphate-buffered saline (PBS) and subsequently centrifuged at 2000 × g for 5 min. Pellets were resuspended in ice-cold Tris buffer (50 mM Tris-HCl, pH 7.4) and

homogenized with an Ultra Turrax homogenizer (IKA-Werke GmbH & Co. KG, Staufen, Germany). Cytosolic and membrane fractions were separated using an Optima LE-80 K ultracentrifuge (Beckman Coulter, Inc., Fullerton, CA) at 100,000 × g for 20 min at 4 °C. This homogenization and centrifugation cycle were repeated a second time. The final pellet was resuspended and homogenized in ice-cold Tris buffer and subsequently aliquoted and stored in 100 μL aliquots at −80 °C. Membrane protein concentrations were determined using a BCA protein determination assay, as described by the manufacturer (Pierce BCA protein assay kit) [24].

2.4. [3H]RO6957022 binding assays

[3H]RO6957022 binding assays have previously been described with the main difference that the incubation temperature was changed to 10 °C for improved separation of kinetic differences [25]. In short, CHOK1_hCB_2bgal membranes were thawed and subsequently homogenized using the Ultra Turrax homogenizer. For experiments with endocannabinoids, membranes were preincubated for 30 min with 50 μM phenylmethylsulfonyl fluoride (PMSF). The reactions were carried out in 100 μL assay buffer (50 mM Tris-HCl (pH 7.4), 0.1% (w/v) bovine serum albumin (BSA)) containing 1 μg of membrane protein and 1.5 nM [3H]RO6957022. Incubations were performed at 10 °C. Therefore, assay buffer, (radio)ligands and membranes were precooled to 10 °C prior to the experiment. Nonspecific binding (NSB) was determined using 10 μM AM630 and vehicle (*i.e.* acetonitrile for endocannabinoids, and DMSO for all other compounds) concentrations were constant and kept < 1% in all samples unless stated otherwise. Total radioligand binding (TB) did not exceed 10% of the amount added to prevent ligand depletion. For all assays, incubations were terminated by rapid vacuum filtration with ice-cold 50 mM Tris-HCl (pH 7.4), 0.1% (w/v) BSA buffer through Whatman GF/C filters using a Filtermate 96-well harvester (PerkinElmer). Filters were dried for at least 30 min at 55 °C and subsequently 25 μL Micro-Scint scintillation cocktail was added per well. Filter-bound radioactivity was measured by scintillation spectrometry using a Microbeta2 2450 counter (PerkinElmer).

2.4.1. Dissociation assays

For all dissociation assays, membranes were pre-incubated with radioligand for 2 h at 10 °C. [3H]RO6957022 dissociation was initiated by addition of 10 μM AM630 as displacer at different time points for 3 h. The allosteric screen was performed in single point dissociation assays by addition of displacer in the absence (control) or presence of 10 μM (f. c.) compound for a total incubation of 27 min (*i.e.* dissociation half-life of the radioligand in this assay). In full curve modulatory dissociation assays, the amount of receptor-bound radioligand was determined at different time points up to 3 h (CBD) or 5 h (CBD-DMH) upon addition of the displacer in the absence (control) or presence of increasing concentrations of CBD-DMH or 10 μM CBD. Final DMSO concentrations were increased to 1.5% to improve solubility. Incubations were terminated and receptor-bound radioactivity was determined as described in section 2.4.

2.4.2. Displacement assays

For displacement assays, membranes were incubated with 10 μM or six increasing concentrations of competing ligand (ranging from 0.01 nM to 10 μM) in the absence (control) or presence of increasing concentrations of CBD-DMH or 3 μM CBD. To prevent precipitation in the assay, the maximum modulatory concentrations of CBD-DMH and CBD were set to 3 μM and all other CBD-DMH concentrations were chosen to be evenly distributed over its displacement curve. The reaction mixture was incubated for 2 h at 10 °C after which incubations were terminated and receptor-bound radioactivity was determined as described in section 2.4.

2.5. [³H]CP55,940 displacement assays

For single point [³H]CP55,940 displacement assays, CHOK1_hCB$_2$bgal membranes were homogenized and diluted to 1.5 μg of membrane protein per well in assay buffer (50 mM Tris-HCl (pH 7.4), 5 mM MgCl$_2$, 0.1% (w/v) BSA). Membranes were incubated with 10 μM of competing ligand in the presence of 1.5 nM [³H]CP55,940. Incubations were for 2 h at 25 °C. NSB was determined using 10 μM AM630 and DMSO concentrations were constant and kept < 1% in all samples. TB did not exceed 10% of the amount added to prevent ligand depletion. Incubations were terminated as described in section 2.4 except using ice-cold wash buffer containing 50 mM Tris-HCl, 5 mM MgCl$_2$ and 0.1% BSA.

2.6. [³⁵S]GTPγS binding assays

G protein activation of CB$_2$R was measured by binding of [³⁵S]GTPγS as previously described [26]. In short, CHOK1_hCB$_2$bgal membrane homogenates (5 μg) were diluted in assay buffer (50 mM Tris-HCl, 5 mM MgCl$_2$, 150 mM NaCl, 1 mM EDTA, 0.05% BSA (w/v) and 1 mM DTT, freshly prepared each day) and supplemented with 5 μg saponin and 1 μM GDP to a total volume of 100 μL. For endocannabinoid samples, the membranes were additionally preincubated for 30 min with 50 μM PMSF. To determine pEC$_{50}$ and E$_{max}$ values, increasing concentrations of ligand of interest (ranging from 0.01 nM to 10 μM) in absence (control) or presence of increasing concentrations of CBD-DMH or 0.3 μM CBD were preincubated for 30 min at rt. To prevent precipitation in the assay, the maximum modulatory concentrations of CBD-DMH and CBD were set to 0.3 μM and all other CBD-DMH concentrations were chosen to be evenly distributed over its displacement curve. Basal activity was determined in the presence of vehicle (*i.e.* acetonitrile for endocannabinoids, and DMSO for all other compounds) or specific CBD-DMH/CBD concentration only and the maximal response was determined by 10 μM CP55,940 or specific ligand of interest. [³⁵S]GTPγS (0.3 nM) was added, and the samples were incubated for 90 min at 25 °C while shaking at 400 rpm. Incubations were terminated as described in section 2.4 except using ice-cold wash buffer containing 50 mM Tris-HCl and 5 mM MgCl$_2$.

2.7. cAMP Hunter™ assays

Inhibition of cAMP production by CB$_2$R stimulation in CB$_2$R-overexpressing cell lines was measured using the cAMP Hunter™ assay enzyme fragment complementation chemiluminescent detection kit as described before and following the manufacturer's protocol (DiscoveRx, Fremont, CA) [27]. Briefly, CHO-K1 cells overexpressing human CB$_2$R were plated into a 96 well plate (10,000 cells/well) and incubated overnight at 37 °C and 5% CO$_2$. Media were aspirated and replaced with 30 μL of cell assay buffer. Cells were treated for 30 min at 37 °C with 15 μL of 3 × dose–response solutions of samples prepared in presence of cell assay buffer containing a 3 × 25 μM NKH477 solution (a water soluble analog of forskolin) to stimulate adenylate cyclase and enhance basal cAMP levels. Following stimulation, cell lysis and cAMP detection were performed as per the manufacturer's protocol. Luminescence was measured using a GloMax Multi Detection System (Promega, Italy).

2.8. PathHunter β-arrestin-2 recruitment assays

β-arrestin-2 recruitment to CB$_2$R was measured using the PathHunter β-arrestin recruitment assay kit as described before [28]. In short, CHOK1_hCB$_2$bgal cells were seeded at a density of 5,000 cells/well in solid white-walled 384-wells plates in culture medium as described in section 2.2 and incubated overnight at 37 °C and 5% CO$_2$. For experiments with endocannabinoids, the cells were preincubated for 30 min at 37 °C and 5% CO$_2$ with 50 μM PMSF. To determine pEC$_{50}$ and E$_{max}$ values, cells were stimulated with increasing concentrations of ligand of interest (ranging from 0.01 nM to 10 μM) in absence (control) or presence of increasing concentrations of CBD-DMH or 1 μM CBD for 90 min at 37 °C and 5% CO$_2$. To prevent precipitation in the assay, the maximum modulatory concentrations of CBD-DMH and CBD were set to 1 μM and all other CBD-DMH concentrations were chosen to be evenly distributed over its displacement curve. Basal activity was determined in the presence of vehicle or specific CBD-DMH/CBD concentration only and the maximal response was determined by 10 μM CP55,940 or specific ligand of interest. Vehicle (*i.e.* acetonitrile for endocannabinoids, and DMSO for all other compounds) concentrations were constant and kept < 1% in all samples. Subsequently, cells were loaded with 12.5 μL detection reagent prepared according to suppliers protocol [29] and incubated for 1 h in the dark at rt to detect ß-galactosidase enzyme activity. Luminescence was measured on an Envision multilabel plate reader (PerkinElmer).

2.9. Data analysis

All experimental data were analyzed using GraphPad Prism 9.0 (GraphPad Software Inc., San Diego, CA). All values obtained are means ± standard deviation (SD) of at least three independent experiments performed in duplicate, unless stated otherwise.

[³H]RO6957022 and [³H]CP55,940 assays were baseline-corrected with NSB and normalized to this value (0%) and TB (100%). Dissociation rate constants (k$_{off}$) were determined by the 'one-phase decay exponential decay' analysis. The half-maximal inhibitory concentrations (pIC$_{50}$) of the agonists in [³H]RO6957022 displacement assays were obtained by non-linear regression analysis of the displacement curves. Values from direct competition curves were further converted into inhibitory constant pK$_i$ using the Cheng-Prusoff equation [30] with the experimentally determined dissociation constant (K$_D$) value 0.78 nM (data not shown). The modulation in apparent affinities was investigated on the level of the pIC$_{50}$ values and the Cheng-Prusoff equation was not applied due to the possibility of CBD-DMH altering the K$_D$ crucial for the analysis.

Functional agonist responses from the [³⁵S]GTPγS binding assays and ß-arrestin-2 recruitment assays were baseline-corrected with the basal activity and normalized to 10 μM of CP55,940 (orthosteric effect) or control response (allosteric modulation). pEC$_{50}$ and E$_{max}$ values were determined using non-linear regression curve fitting 'log(agonist) vs. response'. On reference agonist data the 'three parameters' fit was used, whereas for CBD-DMH and CBD the variable slope (four parameter) fit was applied. This gave freedom to observe both agonistic and allosteric mechanisms of these unknown compounds. Data from the cAMP assay were normalized to NKH477 stimulus alone as 100%. The percentage of response was calculated using the following formula:

$\%response = 100*1 - \frac{meanRLU_{testsample} - meanRLU_{NKH477}}{meanRLU_{vehicle} - meanRLU_{NKH477}}$. pEC$_{50}$ values were determined using non-linear regression curve fitting 'log(agonist) vs. response (three parameters)'.

Differences in pIC$_{50}$ and pEC$_{50}$ values were analyzed using an ordinary one-way ANOVA with Dunnett's multiple comparisons test or an unpaired Student's *t*-test with Welch's correction. Significant differences are displayed as * p < 0.05, ** p < 0.01, *** p < 0.001 and **** p < 0.0001.

3. Results

3.1. Screening of CBD-DMH and proclaimed allosteric modulators of ECS on CB$_2$R

To explore the molecular pharmacological profile of CBD-DMH on CB$_2$R, it was screened in single point displacement assays using inverse agonist [³H]RO6957022 and agonist [³H]CP55,940 along with ten proclaimed ECS modulators for reference (Figs. 1, 2A, Table 1). ZCZ011, GAT211, GAT228, GAT229 and CBD-DMH displaced [³H]RO6957022 between 18 and 42% when tested at 10 μM, whereas ORG27569 and
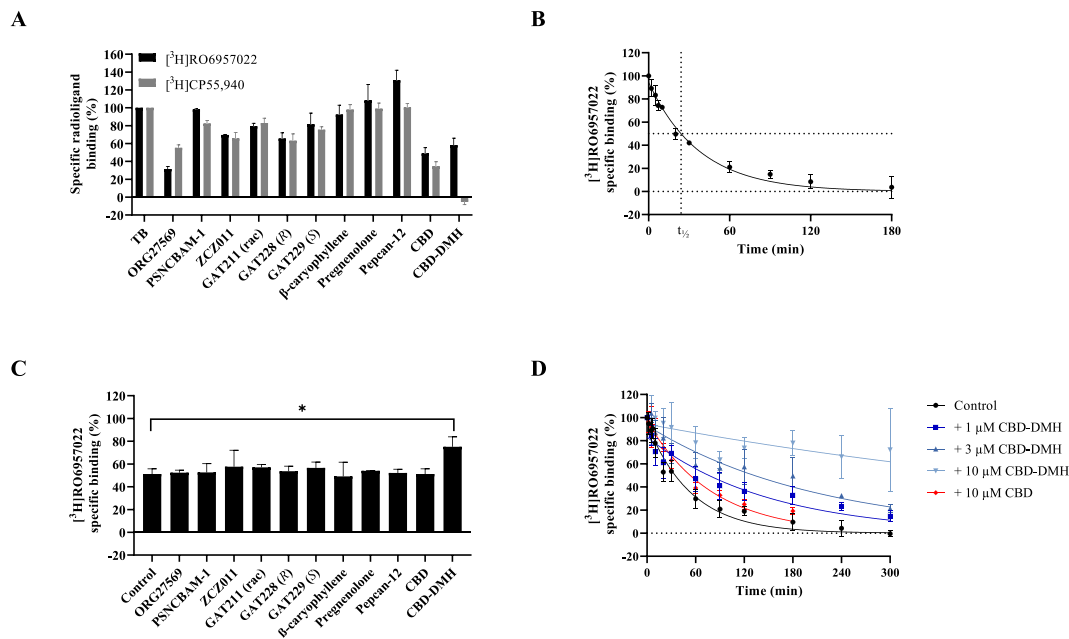
Fig. 2. Screening of reported allosteric modulators of the ECS in radioligand binding assays on hCB$_2$R. (A) Displacement of [^{3}H]RO6957022 or [^{3}H]CP55,940 by 10 μM compound. (B) Dissociation of [^{3}H]RO6957022 from hCB$_2$R at 10 °C with indicated half life time (t$_{1/2}$). (C) Binding of [^{3}H]RO6957022 after 27 min of dissociation (t$_{1/2}$) from hCB$_2$R induced by 10 μM AM630 in the absence (control) or presence of 10 μM of compound. (D). Dissociation curves of [^{3}H]RO6957022 from hCB$_2$R induced by 10 μM AM630 in the absence (control) or presence of increasing concentrations of CBD-DMH or 10 μM CBD. Total binding (TB) of specific radioligand was set to 100%. Data are shown as mean ± SD from at least two (A,C) or three (B,D) independent experiments performed in duplicate.

Table 1
Screening of reported allosteric modulators of the ECS in radioligand binding assays on hCB$_2$R.

Compound	[^{3}H] RO6957022 displacement (%)[a]	[^{3}H] CP55,940 displacement (%)[b]	[^{3}H] RO6957022 binding (%)[c]
Control	N.A.	N.A.	51 ± 5
ORG27569	68 ± 3	45 ± 3	52 ± 2
PSNCBAM-1	2 ± 1	18 ± 4	53 ± 8
ZCZ011	30 ± 1	34 ± 7	58 ± 14
GAT211 (rac)	21 ± 3	17 ± 5	57 ± 2
GAT228 (R)	34 ± 6	37 ± 8	54 ± 4
GAT229 (S)	18 ± 12	25 ± 3	57 ± 5
β-caryophyllene	8 ± 11	2 ± 6	49 ± 12
Pregnenolone	−8 ± 18	1 ± 6	54 ± 0
Pepcan-12	−31 ± 11	0 ± 4	52 ± 3
CBD	51 ± 6	65 ± 5	51 ± 5
CBD-DMH	42 ± 8	105 ± 3	75 ± 9*

Values represent the mean ± SD of at least two individual experiments performed in duplicate. One-way ANOVA with Dunnett's multiple comparisons test was used to analyze differences in specific binding compared to control (*p < 0.05). N.A. is not applicable.

[a] Percentage [^{3}H]RO6957022 displacement from hCB$_2$R in the presence of 10 μM compound after 2 h.

[b] Percentage [^{3}H]CP55,940 displacement from hCB$_2$R in the presence of 10 μM compound after 2 h.

[c] Percentage [^{3}H]RO6957022 binding after 27 min of dissociation from hCB$_2$R induced by 10 μM AM630 in absence (control) or presence of 10 μM compound.

CBD displaced the radioligand more than 50% at this concentration. PSNCBAM-1, ß-caryophyllene and pregnenolone did not displace [^{3}H]RO6957022 at all and pepcan-12 slightly increased the specific binding of [^{3}H]RO6957022. Using [^{3}H]CP55,940, six compounds displaced the radioligand between 17 and 45%, but only 10 μM CBD and CBD-DMH displaced the agonistic radioligand for 65% and 105%, respectively. Compounds ß-caryophyllene, pregnenolone and pepcan-12 did not influence [^{3}H]CP55,940 binding.

To investigate allosteric effects of CBD-DMH and the ECS modulators, radioligand dissociation assays were executed. For a quick screening of all compounds, a single point [^{3}H]RO6957022 dissociation assay was designed. In the presence of 10 μM AM630, dissociation of [^{3}H]RO6957022 followed a monophasic decay until full dissociation was reached after approximately 180 min, where its dissociation half-life (t$_{1/2}$) was 27 min, *i.e.* the point where 50% of the radioligand was still bound (Fig. 2B). Subsequently, all eleven compounds were screened in a single point [^{3}H]RO6957022 dissociation assay at t$_{1/2}$ of 27 min of dissociation, *i.e.* the time point that equally allows for the observation of an increase or decrease in radioligand dissociation rate (Fig. 2C). Only CBD-DMH significantly increased the specific binding of [^{3}H] RO6957022 to 75 ± 9% compared to 51 ± 5% of control (Fig. 2C, Table 1). Interestingly, close analog CBD did not change the specific binding (51 ± 5%). To further quantify these effects, a full curve dissociation in the presence of CBD-DMH and CBD was performed (Fig. 2D, Table 2). CBD-DMH drastically altered the dissociation of [^{3}H] RO6957022, which could not be quantified in the three hour timeframe. Therefore, the incubation time was extended to five hours and time points were distributed to capture the full response. The dissociation rate constant (k$_{off}$) of [^{3}H]RO6957022 was significantly reduced in the presence of 1 and 3 μM CBD-DMH with k$_{off}$ values of 0.007 ± 0.002

Table 2
Dissociation rate constants in the absence and presence of increasing concentrations of CBD-DMH or 10 μM CBD in [^{3}H] RO6950722 dissociation assays.

Modulator	k$_{off}$ (min^{-1})
Control	0.019 ± 0.005
+ 1 μM CBD-DMH	0.007 ± 0.002***
+ 3 μM CBD-DMH	0.005 ± 0.001***
+ 10 μM CBD-DMH	N.D.
+ 10 μM CBD	0.013 ± 0.001*

Values represent the mean ± SD of at least three individual experiments performed in duplicate. One-way ANOVA with Dunnett's multiple comparisons test was used to analyze differences in k$_{off}$ compared to vehicle (*p < 0.05, ** p < 0.01, *** p < 0.001, **** p < 0.00001). N.D. is not determined.

min^{-1} and 0.005 ± 0.001 min^{-1}, respectively, compared to 0.019 ± 0.005 min^{-1} in the control condition. Furthermore, even after 5 h incubation in the presence of 10 μM CBD-DMH this parameter could no longer be quantified, as the radioligand's dissociation was extremely impaired. The k_{off} of [^{3}H]RO6957022 in the presence of 10 μM CBD was also significantly reduced to 0.013 ± 0.001 min^{-1}, but this was less than 2-fold from control and is therefore not considered biologically relevant (Fig. 2D, Table 2).

Together, the results from the screening assays suggest a weak competitive interaction of ORG27569 and CBD with [^{3}H]CP55,940 at CB$_2$R, while CBD weakly and CBD-DMH more potently displaced [^{3}H] RO6957022. Interestingly, CBD-DMH is also an allosteric enhancer of [^{3}H]RO6957022 binding at CB$_2$R, indicating a second possible binding site. Notably, none of the other compounds exhibit evident allosteric enhancement or inhibition. Therefore, the binding mechanism of CBD-DMH is further explored, while taking CBD along as control.

3.2. Affinity of orthosteric reference ligands in the absence or presence of CBD-DMH and CBD

The competitive behavior of CBD-DMH and CBD was further investigated in full curve displacement assays with [^{3}H]RO6957022. CBD-DMH displayed a pK$_i$ value of 6.46 ± 0.20, while a remaining 20% of [^{3}H]RO6957022 was not displaced (Fig. 3A, Table 3). CBD only showed

Table 3

Apparent affinity (pK$_i$) of CBD-DMH or apparent affinity (pIC$_{50}$) of orthosteric ligands in the absence or presence of CBD-DMH and CBD as determined in [^{3}H] RO6957022 displacement assays.

Modulator	CBD-DMH	RO6957022	CP55,940	2-AG	AEA
Control	6.46 ± 0.20	8.39 ± 0.49	8.78 ± 0.28	6.20 ± 0.16	5.58 ± 0.16
+ 0.03 μM CBD-DMH	N.A.	8.30 ± 0.32	8.62 ± 0.26	6.14 ± 0.06	5.49 ± 0.17
+ 0.3 μM CBD-DMH	N.A.	7.97 ± 0.12	8.52 ± 0.63	6.06 ± 0.21	5.57 ± 0.25
+ 3 μM CBD-DMH	N.A.	6.99 ± 0.55**	7.04 ± 0.92*	5.01 ± 0.20****	4.47 ± 0.50**
+ 3 μM CBD	N.A.	8.04 ± 0.45	8.60 ± 0.36	5.88 ± 0.05	5.45 ± 0.14

Values represent the mean ± SD of at least three individual experiments performed in duplicate. pK$_i$ (CBD-DMH) and pIC$_{50}$ values of orthosteric reference ligands in the absence (control) or presence of increasing concentrations of CBD-DMH or 3 μM CBD were obtained from [^{3}H]RO6957022 displacement assays on membranes stably expressing hCB$_2$R. One-way ANOVA with Dunnett's multiple comparisons test was used to analyze differences in pIC$_{50}$ compared to control (*$p < 0.05$, ** $p < 0.01$, *** $p < 0.001$, **** $p < 0.00001$). N.A. is not applicable.
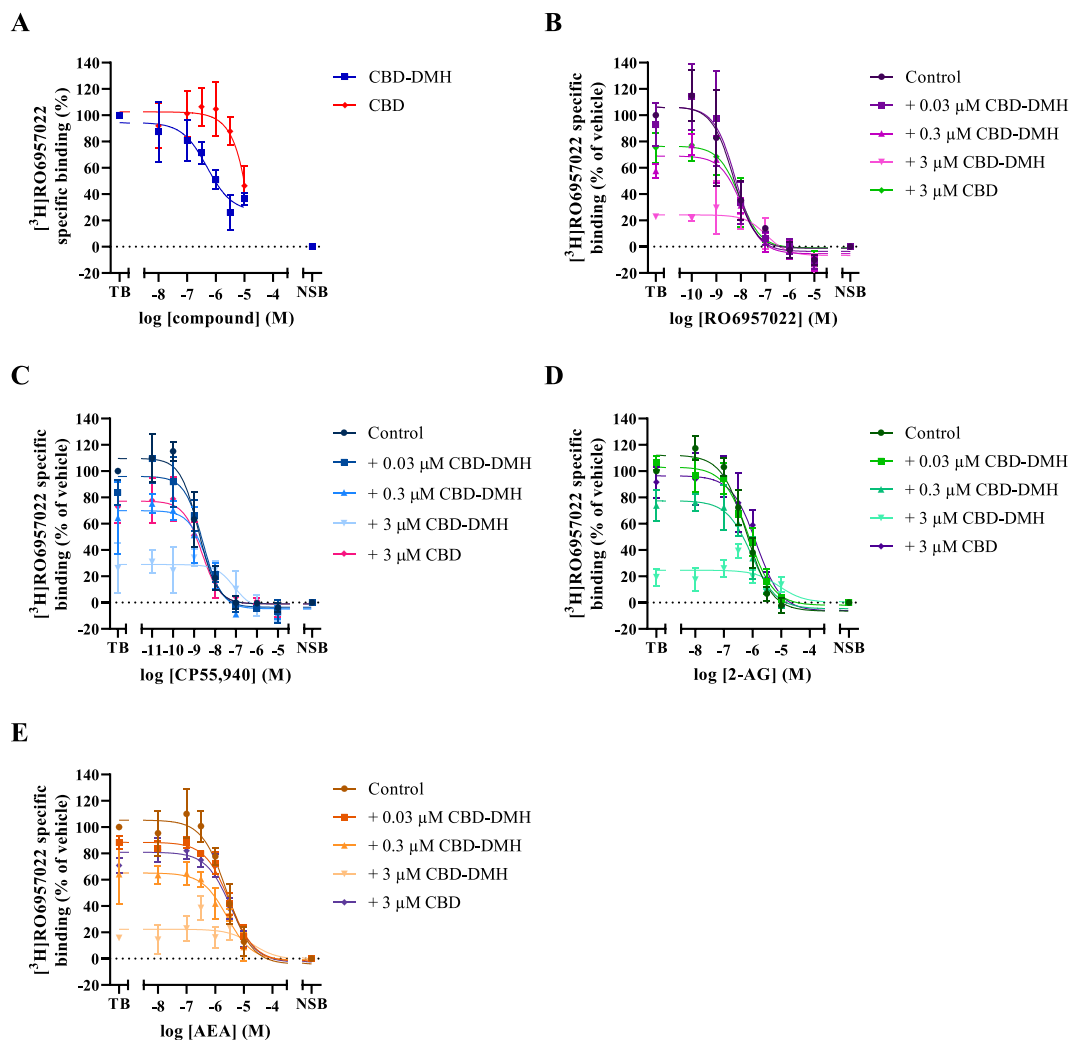
Fig. 3. Affinity and modulation of affinity of orthosteric ligands by CBD-DMH and CBD. (A) [^{3}H]RO6957022 displacement by CBD-DMH and CBD. [^{3}H]RO6950722 displacement by (B) orthosteric inverse agonist RO6957022, orthosteric agonists (C) CP55,940, (D) 2-AG and (E) AEA in the absence (control) or presence of increasing concentrations of CBD-DMH or 3 μM CBD. Data are shown as mean ± SD from at least three independent experiments performed in duplicate.

weak displacement at 10 μM, as such its affinity for CB_2R could not be determined (Fig. 3A).

As allosteric modulation can be probe-dependent, the modulating effect of CBD-DMH and CBD was investigated on the binding of various reference ligands. Specifically, modulation of CP55,940 (which was also used as a radioligand in the screen, Fig. 2A), and two endogenous agonists, i.e. 2-AG and AEA, was evaluated and compared to their effect on unlabeled RO6957022. To this end, [^{3}H]RO6957022 displacement assays in the absence or presence of increasing concentrations of CBD-DMH or 3 μM CBD were performed (Fig. 3, Table 3). The control conditions reflected the increased displacement of [^{3}H]RO6957022 in the presence of increasing concentrations of CBD-DMH from 0% up to 80% and 20% displacement in the presence of 3 μM CBD, which corresponded well to their values in the displacement curves (Fig. 3).

For both inverse agonist RO6957022 and agonist CP55,940 a trend in decreased apparent affinity (pIC_{50}) was found in the presence of increasing concentrations of CBD-DMH (Fig. 3C,D, Table 3). Specifically, their apparent affinities were significantly decreased in the presence of the highest concentration of 3 μM CBD-DMH by 25- and 54-fold, respectively. Similarly, the apparent affinities of endogenous agonists 2-AG and AEA were significantly reduced in the presence of 3 μM CBD-DMH by 15- and 13-fold compared to control condition. However, 3 μM CBD did not statistically significant affect the apparent affinity of any orthosteric ligand (Fig. 3C-F, Table 3). This further confirms the lack of allosteric modulation by CBD at CB_2R, whereas CBD-DMH impaired the apparent affinity of the inverse agonist, synthetic agonist, and endogenous agonists at CB_2R. Nevertheless, CBD-DMH also competes with RO6957022 for binding to CB_2R.

3.3. $G\alpha_i$ protein activation by CBD-DMH and modulation of orthosteric reference agonists in the absence or presence of CBD-DMH and CBD

[^{35}S]GTPγS binding assays were performed to investigate $G\alpha_i$ protein activation by CBD-DMH and CBD. CBD-DMH behaved as a partial agonist with a pEC_{50} value of 7.42 ± 0.14 and E_{max} value of $69 \pm 5\%$ compared to full agonist CP55,940 (Fig. 4A, Table 4). CBD did not induce any $G\alpha_i$ protein activation on CB_2R. Furthermore, this agonistic

effect of CBD-DMH was also observed in a cAMP assay with a potency of 8.05 ± 0.28, i.e. cAMP production was inhibited by CBD-DMH at CB_2R (Table 4).

To evaluate the modulatory effect of CBD-DMH and CBD on $G\alpha_i$ protein activation induced by orthosteric agonists CP55,940, 2-AG and AEA, functional [^{35}S]GTPγS binding assays were performed in the absence and presence of increasing concentrations of CBD-DMH and 0.3 μM CBD (Fig. 4, Table 4). Firstly, the basal conditions reflected the partial agonistic behavior of CBD-DMH for $G\alpha_i$ protein activation, which was not observed for CBD (Fig. 4). Secondly, a dose-dependent negative modulation of CP55,940-induced $G\alpha_i$ protein activation was observed in the presence of CBD-DMH (Fig. 4B). Specifically, pEC_{50} values were significantly decreased from 8.90 ± 0.45 to 7.01 ± 0.46 in the presence of 0.3 μM CBD-DMH (Table 4). On the other hand, CBD did not modulate CP55,940 activation of CB_2R. Neither CBD-DMH nor CBD affected the maximum activation level by CP55,940. Although not statistically significant, a trend was observed that CBD-DMH dose-dependently decreased the potency of 2-AG, without affecting its maximum activation (Fig. 4C, Table 4). CBD did neither statistically significant affect the potency of 2-AG nor AEA (Fig. 4C, D, Table 4). Finally, AEA-induced G protein activation was differently impacted by CBD-DMH compared to the other agonists, as the level of activation induced by CBD-DMH was higher than AEA efficacy (Fig. 4A). Hence, the increasing concentrations of AEA caused the level of CBD-DMH activation to be brought back to the maximal AEA activation level. Noteworthy, the lowest CBD-DMH concentration tested (0.03 μM) resulted in a level of G protein activation equal to AEA's efficacy, i.e. resulting in a flat dose–response curve.

In conclusion, we observed partial agonism of CBD-DMH, but not CBD, in G protein activation and cAMP assays on CB_2R. Moreover, CBD-DMH, but not CBD, also negatively modulated agonist-induced $G\alpha_i$ protein activation.

3.4. β-arrestin-2 recruitment by CBD-DMH and modulation of orthosteric reference agonists in the absence or presence of CBD-DMH and CBD

Another functional assay was performed to investigate the effect of CBD-DMH and CBD on β-arrestin-2 recruitment to CB_2R. CBD-DMH
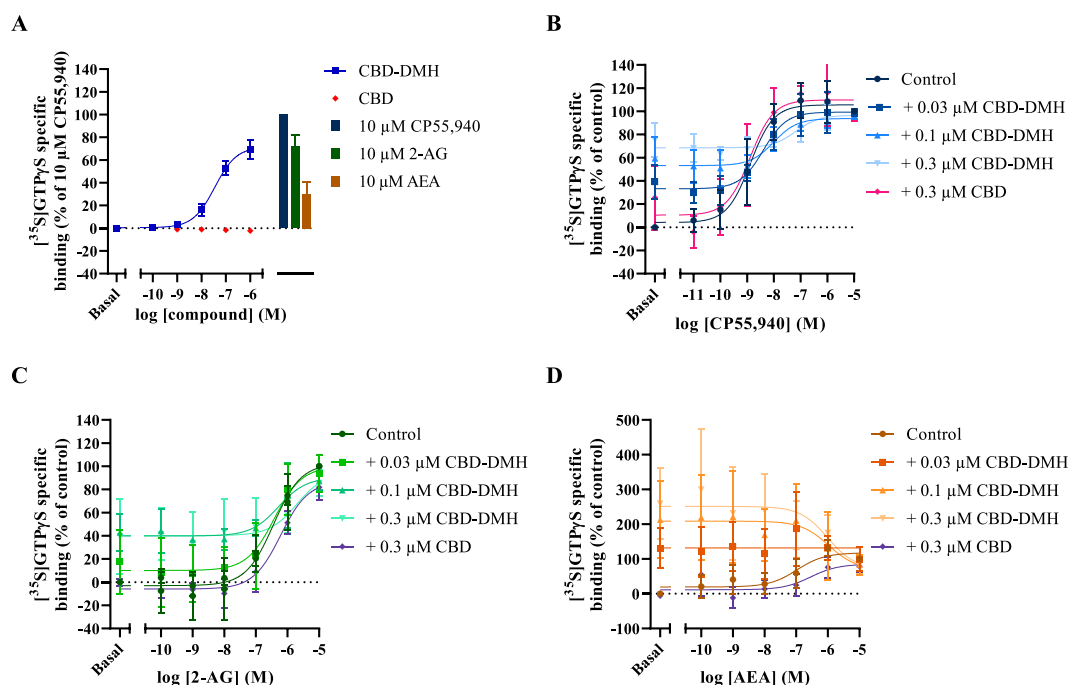
Fig. 4. G protein activation and modulation thereof by CBD-DMH and CBD. (A) [^{35}S]GTPγS binding by CBD-DMH and CBD compared to full agonist CP55,940. Modulation of orthosteric agonists (B) CP55,940, (C) 2-AG and (D) AEA-induced [^{35}S]GTPγS binding in the absence (control) or presence of increasing concentrations of CBD-DMH or 0.3 μM CBD. Data are shown as mean ± SD from at least three independent experiments performed in duplicate.

Table 4

Potency (pEC$_{50}$) and maximum activation (E$_{max}$) of orthosteric ligands in the absence or presence of CBD-DMH and CBD determined in functional assays.

Assay	Agonist Modulator	CBD-DMH pEC$_{50}$	E$_{max}$ (%)	CP55,940 pEC$_{50}$	E$_{max}$ (%)	2-AG pEC$_{50}$	E$_{max}$ (%)	AEA pEC$_{50}$	E$_{max}$ (%)
[^{35}S] GTPγS binding assay	Control	7.42 ± 0.14	69 ± 5	8.90 ± 0.45	106 ± 10	6.39 ± 0.26	105 ± 6	7.03 ± 0.34	123 ± 11
	+ 0.03 μM CBD-DMH	N.A.	N.A.	8.42 ± 0.01	99 ± 13	6.30 ± 0.41	102 ± 7	N.D.	100 ± 34[#]
	+ 0.1 μM CBD-DMH	N.A.	N.A.	8.01 ± 0.02*	94 ± 4	6.18 ± 0.83	98 ± 16	N.D.	84 ± 29[#]
	+ 0.3 μM CBD-DMH	N.A.	N.A.	7.01 ± 0.46****	98 ± 3	5.63 ± 0.32	100 ± 20	N.D.	83 ± 27[#]
	+ 0.3 μM CBD	N.A.	N.A.	9.00 ± 0.47	110 ± 12	6.27 ± 0.46	89 ± 16	6.52 ± 0.14	86 ± 20
cAMP assay	Control	8.05 ± 0.28	N.A.	N.A.	N.A.	N.A.	N.A.	N.A.	N.A.
ß-arrestin-2 recruitment assay	Control	6.92 ± 0.13	47 ± 15	8.35 ± 0.12	99 ± 3	5.68 ± 0.09	100 ± 17[#]	6.53 ± 0.13	98 ± 3
	+ 0.1 μM CBD-DMH	N.A.	N.A.	8.50 ± 0.11	115 ± 9	5.32 ± 0.76	104 ± 13[#]	6.51 ± 0.32	102 ± 8
	+ 0.3 μM CBD-DMH	N.A.	N.A.	8.46 ± 0.06	100 ± 5	5.58 ± 0.40	111 ± 29[#]	6.41 ± 0.82	103 ± 14
	+ 1 μM CBD-DMH	N.A.	N.A.	8.28 ± 0.32	115 ± 13	5.64 ± 0.28	104 ± 14[#]	N.D.	105 ± 21
	+ 1 μM CBD	N.A.	N.A.	8.43 ± 0.12	72 ± 11	5.54 ± 0.16	103 ± 23[#]	6.48 ± 0.31	107 ± 18

Values represent the mean ± SD of at least three individual experiments performed in duplicate. Potency (pEC$_{50}$) and maximum effect (E$_{max}$) or effect at 10 μM values of orthosteric reference ligands (#) in the absence (control) or presence increasing concentrations of CBD-DMH or CBD were obtained from [^{35}S]GTPγS binding, cAMP or ß-arrestin-2 recruitment assays on membranes or cells stably expressing hCB$_2$R, respectively. The percentage maximum effect at 10 μM was calculated compared to the top of the control curves. One-way ANOVA with Dunnett's multiple comparisons test was used to analyze differences in pEC$_{50}$ compared to control (*p < 0.05, ** p < 0.01, *** p < 0.001, **** p < 0.00001). N.D. is not determined. N.A. is not applicable.

behaved as a partial agonist on ß-arrestin-2 recruitment with a pEC$_{50}$ value of 6.92 ± 0.13 and 47 ± 15% activation compared to CP55,940 (Fig. 5A, Table 4). Furthermore, CBD did not induce ß-arrestin-2 recruitment to CB$_2$R.

The modulatory effect of CBD-DMH and CBD on ß-arrestin-2 recruitment by CP55,940, 2-AG and AEA to CB$_2$R was further examined in this assay (Fig. 5, Table 4). As expected, the basal conditions reflected the partial agonism of CBD-DMH on ß-arrestin-2 recruitment to CB$_2$R (Fig. 5A). Similar to the G protein activation results, no statistically significant modulation by CBD was detected for CP55,940, 2-AG or AEA-induced ß-arrestin-2 recruitment (Fig. 5B-D, Table 4). CBD-DMH did not induce a dose-dependent negative modulation of CP55,940, 2-AG or AEA-induced ß-arrestin-2 recruitment, in contrast to G protein activation results (Fig. 5B-D, Table 4). Interestingly, modulation of AEA-induced ß-arrestin-2 recruitment by highest concentration of 1 μM CBD-DMH could not be determined due to an already maximal

activation of the receptor by CBD-DMH.

Altogether, we found partial agonism of CBD-DMH, but not CBD, in ß-arrestin-2 recruitment assays similar to the G protein activation assays. However, unlike in G protein activation assays, no modulation of CBD-DMH or CBD was observed on any agonist-induced ß-arrestin-2 recruitment to CB$_2$R.

4. Discussion and conclusion

For centuries, components from *Cannabis sativa*, such as CBD, have been used for medicinal purposes [6]. Recently, the FDA approved Epidiolex®, a pure CBD solution, for the treatment of severe pediatric seizure disorders [5,9]. Furthermore, CBD has attracted the attention of the general public as a wonder drug that can be obtained over the counter. However, its pharmacological profile is still not fully understood and seems to be attributed to polypharmacology, *i.e.* activity at
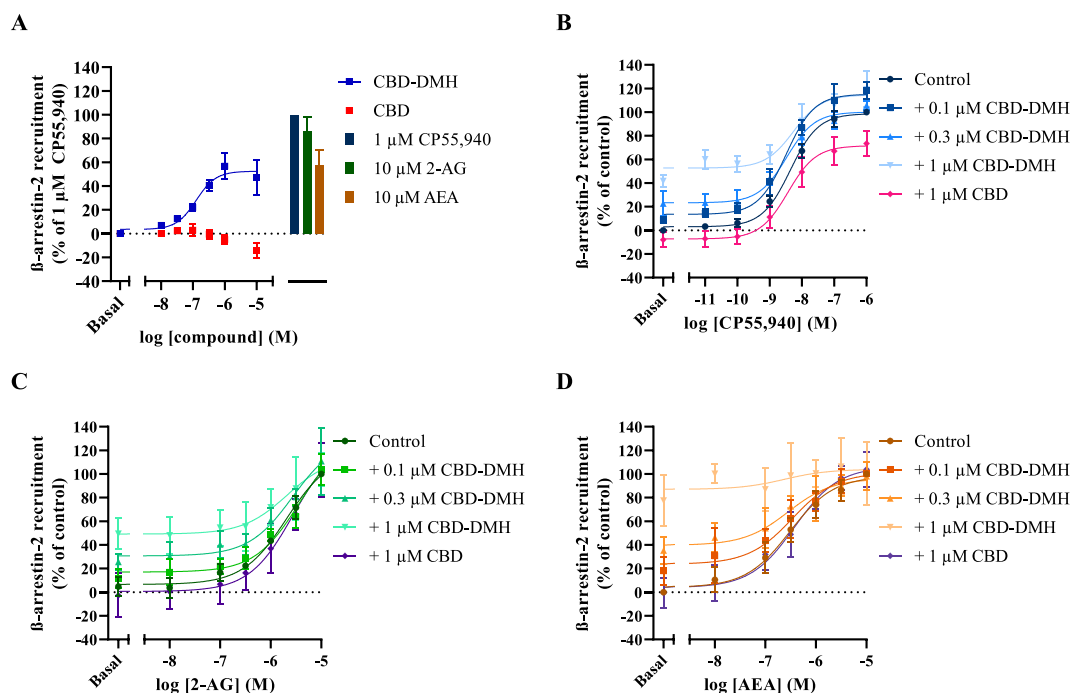

Fig. 5. ß-arrestin-2 recruitment and the modulation thereof by CBD-DMH and CBD. (A) ß-arrestin-2 recruitment by CBD-DMH and CBD compared to full agonist CP55,940. Modulation of agonists (B) CP55,940, (C) 2-AG and (D) AEA-induced ß-arrestin-2 recruitment in the absence (control) or presence of increasing concentrations of CBD-DMH or 1 μM CBD. Data are shown as mean ± SD from at least three independent experiments performed in duplicate.

multiple targets [10–13,31]. Meanwhile, synthetic CBD derivates have been synthesized including CBD-DMH [14]. CBD-DMH showed anti-inflammatory effects in various *in vitro* models, and furthermore showed efficacy in an *in vivo* arachidonic acid-induced inflammation model [15–17,19]. Nevertheless, the exact molecular mechanism of CBD-DMH remains unknown but has been hypothesized to be mediated by various proteins including CB_2R [20–22]. Therefore, we aimed to further characterize the molecular pharmacological effect of CBD-DMH on this receptor. One of the proposed mechanisms of CBD-DMH on CB_2R has been attributed to allosteric modulation [22]. Allosteric modulation, *i.e.* binding of a ligand at a binding site distinct from the orthosteric site, presents several advantages over orthosteric targeting of receptors [32]. This includes the lack of intrinsic agonistic properties indicating allosteric modulators can only modify the binding or signaling of a second ligand, *e.g.* the endogenous ligand. Furthermore, allosteric modulators bear the possibility of a higher subtype selectivity [32,33]. This class of molecules might present a different strategy for targeting CB_2R.

To investigate the allosteric behavior of CBD-DMH, radioligand binding dissociation assays were performed in which commercially available proclaimed ECS modulators were taken along for reference (Fig. 1) [23]. Alteration of the dissociation rate constant (k_{off}) of an orthosteric ligand has been described as a typical hallmark of allosteric interactions and can consequently lead to altered affinity and/or potency of the orthosteric ligand at the receptor [32,34]. We screened CBD-DMH and the proclaimed modulators of the ECS in a single point dissociation assay at CB_2R for a quick insight into their dissociation modulating properties (Fig. 2C, Table 1) [35]. CB_1R allosteric modulators ORG27569, PSNCBAM-1, ZCZ011, GAT211 (rac), GAT229 (*S*), and pregnenolone did not alter radioligand binding in these assays, which confirmed their lack of allosteric interaction with CB_2R [23]. Previously reported CB_2R negative allosteric modulators (NAMs) ß-caryophyllene and CBD, and positive allosteric modulator (PAM) pepcan-12 did not change the binding profile in our assays [36–38]. To the best of our knowledge, dissociation experiments to identify the allosteric mechanism have only been performed for ß-caryophyllene and pepcan-12 using [³H]CP55,940 [37,38]. The use of a biphasic radioligand such as [³H]CP55,940 may complicate the determination of accurate kinetic parameters for unlabeled ligands due to the preference for different binding states [39]. This issue is circumvented in our assays by using the monophasic [³H]RO6957022. Furthermore, pepcan-12 did not induce a statistically significant shift in agonist potency in [³⁵S]GTPγS or cAMP assays [38]. Intriguingly, several studies report agonistic behavior of ß-caryophyllene by showing affinity for CB_2R and G protein mediated signaling [40,41]. As we aimed to investigate allosterism in this project (which we did not observe), this compound was not taken along in sequential functional studies.

The only compound allosterically affecting the binding of the radioligand on CB_2R was CBD-DMH (Fig. 2C, Table 1). Therefore, the allosteric modulation by CBD-DMH was further investigated in a full curve dissociation assay (Fig. 2D, Table 2). A dose-dependent decrease of [³H]RO6957022 binding was observed in the presence of CBD-DMH and further quantified by significantly reduced k_{off} values, which corroborates an allosteric enhancing effect on inverse agonist RO6957022 at CB_2R [32,35]. Of note, CBD was included in this and all consecutive assays as control compound next to CBD-DMH. Examination of CBD showed no statistically significant allosteric modulation (Fig. 2A), very weak competitive binding (Fig. 3A) but no potency on CB_2R (Fig. 4A, 5A, Table 3, 4). Evidently, CBD might bind orthosteric to CB_2R, but with a very low, non-detectable potency in all our assays, which contrasts with previous assumptions that CBD acts as a partial agonist or allosteric modulator at CB_2R [22,42].

The modulating effect of CBD-DMH was further investigated on the affinity and potency of reference orthosteric ligands in various binding and functional assays. The orthosteric ligands used in this study were inverse agonist RO6957022, reference orthosteric agonist CP55,940 and endogenous agonists 2-AG and AEA to account for potential probe

dependence of CBD-DMH, *i.e.* differential effects on different (types of) ligands (Fig. 1) [33]. The inclusion of the endocannabinoids to our study is a valuable addition since this reflects physiological conditions and provides insight into how physiological effects might be altered [32]. A negative allosteric modulation phenotype of CBD-DMH was found in G protein activation assays in which the potency of CP55,940 was significantly reduced with increasing concentrations of CBD-DMH (Fig. 4B, Table 4). Although not statistically significant, a similar effect by CBD-DMH was observed on the potency of 2-AG (Fig. 4C, Table 4). The modulation of AEA-mediated G protein activation was less apparent due to the higher level of partial agonism of CBD-DMH compared to AEA, which probably overshadows the allosteric action on potency (Fig. 4A,D, Table 4). However, in the presence of various concentrations of CBD-DMH, we observed a higher G protein activation than by AEA alone, where in combination with higher concentrations of AEA the maximal AEA level was observed (Fig. 4D). Together, this suggests that CBD-DMH is a NAM for G protein activation by CB_2R agonists.

Nonetheless, this allosteric effect of CBD-DMH was not sustained in ß-arrestin-2 recruitment assays (Fig. 4B-D, Table 4), which might indicate that CBD-DMH behaves as a biased allosteric modulator, *i.e.* demonstrating preference for modulating one pathway over another [43]. In the study by Tham *et al.*, CBD-DMH was described as a PAM of CP55,940-dependent cAMP inhibition in contrast to the NAM effect on upstream G protein activation found in our study [22]. Secondly, pathway-specific allostery was described with a NAM effect on CP55,940-dependent ß-arrestin-1 recruitment. It is important to note that in this specific study, recruitment of ß-arrestin-1 was investigated in contrast to ß-arrestin 2 in our study. It has been previously described that ß-arrestin-1 has a weaker affinity for CB_2R than ß-arrestin-2, which might suggest different signaling mechanisms and could therefore be differently impacted by binding of CBD-DMH [44]. Even though we did not find a pronounced effect on ß-arrestin-2 recruitment to CB_2R, we also found a pathway-specific allostery between the G protein and ß-arrestin-2 signaling. Importantly, our experiments also highlight the importance of including different chemotypes and types of agonists, *i.e.* agonists and inverse agonists, for investigating probe dependence [45]. Namely, G protein activation by agonists CP55,940 and 2-AG was negatively impacted by CBD-DMH, whereas inverse agonist RO6957022 binding was positively modulated in dissociation studies. Furthermore, these results might be a first indication towards transducer dependency and a biased allosteric effect of CBD-DMH towards G protein activation over ß-arrestin-2 recruitment [43].

While studying the allosteric behavior of CBD-DMH, we also observed competitive or agonistic behavior in several assays. We found competitive displacement of the highest concentration of CBD-DMH with both [³H]RO6957022 and [³H]CP55,940 (Fig. 2A, Table 1). This was further quantified by a low affinity of CBD-DMH for CB_2R in displacement studies, which suggests that CBD-DMH competes with [³H]RO6957022 for the orthosteric binding site (Fig. 3A, Table 3). Although, not further analyzed, Tham *et al.* also found this competitive binding of CBD-DMH with [³H]CP55,940 and a similar low affinity is previously reported with [³H]-HU-243 to CB_2R [20,22]. Interestingly, the binding could not be fully inhibited in our studies (Fig. 3A, Table 3), which is indicative of the formation of a ternary complex of binding of [³H]RO6957022 to the orthosteric site, while CBD-DMH occupies the allosteric site [35,46].

For all tested reference ligands, a decreased apparent affinity was observed in presence of the highest concentration (3 µM) of CBD-DMH (Fig. 3B-E, Table 3), which further highlights the competitive interaction at the orthosteric binding site. The different conclusions obtained from the [³H]RO6957022 dissociation and displacement assays with regard to CBD-DMH's mechanism of action highlight the importance of employing both these assays, as these expose the allosteric and competitive interactions by CBD-DMH, respectively.

The agonistic effect of CBD-DMH was further observed in the various functional assays, where CBD-DMH elicited partial G protein activation

and ß-arrestin-2 recruitment compared to full agonist CP55,940 with moderate pEC_{50} values and hill slopes close to unity (Fig. 4A, 5A, Table 4). No agonistic effect of CBD-DMH on cAMP inhibition was described in the study by Tham *et al.,* but the apparent upward shift of the CP55,940 curve in the presence of increasing concentrations of CBD-DMH would compare to the agonistic effect we also observed and quantified for CBD-DMH on NKH477-induced inhibition of cAMP levels (Table 4) [20]. Our results together stress the duality of CBD-DMH, which is not a pure allosteric modulator, but rather a NAM-agonist due to having two different interactions with CB_2R from which it modulates and activates the receptor [47].

Ligands with two different binding interactions have previously been described for the muscarinic M_2 receptor, where bitopic ligands might adopt a dualsteric binding mode, bridging the orthosteric and allosteric site or purely bind to the allosteric binding site [46]. This allosteric binding pocket has been crystallized for the muscarinic M_2 receptor and sits directly above the orthosteric site [48]. Recently, a study by Yuan *et al.* identified seven potential allosteric sites for CB_2R of which 'site H' was the most promising binding site, which resembles the allosteric site from the M_2 receptor and is close to the orthosteric binding pocket of CB_2R [49]. This site located just above the orthosteric pocket has also been referred to as the extracellular vestibule, ligand entry site or outer vestibule. It is a region in which ligands might pre-engage before moving deeper into the orthosteric binding pocket. Nevertheless, allosteric ligands could bind here without continuing to the orthosteric pocket and execute allosteric actions such as changing the orthosteric ligand-binding kinetics [34,50]. The duality of CBD-DMH described in this paper can be well explained by it having interactions at a yet to be identified allosteric binding site, but also by its binding to the orthosteric site. These orthosteric interactions might be directed by the dimethylheptyl moiety that CBD-DMH has opposed to CBD's pentyl chain. These side chain substitutions generally enhance the activity of cannabinoids [18]. Evidently, it is a common structural feature for CB_2R agonists such as CP55,940, HU308 and HU910 and is described to interact with various amino acids in the orthosteric binding pocket [26]. To dive further into the exact binding mechanism of CBD-DMH at CB_2R, structural elucidation of CB_2R in conjunction with CBD-DMH by docking and molecular dynamic studies could be performed. These should be supported with *in vitro* mutagenesis studies for validation of resultant predicated positions. Together this might aid in obtaining a better idea of the dual pharmacology of CBD-DMH at CB_2R.

In conclusion, this study provides a dual profile of CBD-DMH with both allosteric and orthosteric effects on CB_2R, although it does not identify the exact binding site(s) of CBD-DMH. Interestingly, CBD-DMH partially activates both G protein and ß-arrestin-2 recruitment, while it is a PAM for an inverse agonist, and a NAM for synthetic and endogenous agonists. In case of the latter, it only modulates G protein activation and not ß-arrestin-2 recruitment suggesting a biased allosteric mechanism. Furthermore, in these robust fundamental assays we could not confirm any potent interaction of CBD with CB_2R. Hence, the beneficial effects of CBD can still be attributed to polypharmacology, but most likely not via CB_2R. Together, this study invites further research into identifying the dual molecular pharmacology of CBD-DMH at CB_2R, which might provide a new class of molecules targeting CB_2R.

CRediT authorship contribution statement

Jara Bouma: Conceptualization, Methodology, Investigation, Formal analysis, Data curation, Visualization, Writing – original draft. **Jeremy D. Broekhuis:** Investigation. **Cas van der Horst:** Investigation. **Poulami Kumar:** Investigation, Formal analysis. **Alessia Ligresti:** Writing – review & editing, Supervision. **Mario van der Stelt:** Conceptualization, Writing – review & editing, Supervision. **Laura H. Heitman:** Conceptualization, Writing – review & editing, Supervision, Project administration, Funding acquisition.

Declaration of Competing Interest

The authors declare that they have no known competing financial interests or personal relationships that could have appeared to influence the work reported in this paper.

Data availability

Data will be made available on request.

Acknowledgements

References

[1] A.C. Howlett, F. Barth, T.I. Bonner, G. Cabral, P. Casellas, W.A. Devane, C.C. Felder, M. Herkenham, K. Mackie, B.R. Martin, R. Mechoulam, R.G. Pertwee, International Union of Pharmacology. XXVII. Classification of cannabinoid receptors, Pharmacol Rev. 54 (2002) 161–202. https://doi.org/10.1124/pr.54.2.161.

[2] V. Di Marzo, M. Bifulco, L. De Petrocellis, The endocannabinoid system and its therapeutic exploitation, Nat Rev Drug Discov. 3 (2004) 771–784, https://doi.org/10.1038/nrd1495.

[3] M.S. Ibsen, M. Connor, M. Glass, Cannabinoid CB_1 and CB_2 Receptor Signaling and Bias, Cannabis Cannabinoid Res. 2 (2017) 48–60, https://doi.org/10.1089/can.2016.0037.

[4] R.G. Pertwee, A.C. Howlett, M.E. Abood, S.P.H. Alexander, V. Di Marzo, M.R. Elphick, P.J. Greasley, H.S. Hansen, G. Kunos, K. Mackie, R. Mechoulam, R.A. Ross, International Union of Basic and Clinical Pharmacology. LXXIX. Cannabinoid Receptors and Their Ligands: Beyond CB_1 and CB_2, Pharmacol Rev. 62 (2010) 588–631. https://doi.org/10.1124/PR.110.003004.

[5] B. Brennecke, T. Gazzi, K. Atz, J. Fingerle, P. Kuner, T. Schindler, G. de Weck, M. Nazaré, U. Grether, Cannabinoid receptor type 2 ligands: An analysis of granted patents since 2010, Pharm Pat Anal. 10 (2021) 111–163, https://doi.org/10.4155/ppa-2021-0002.

[6] R. Mechoulam, L.O. Hanuš, R. Pertwee, A.C. Howlett, Early phytocannabinoid chemistry to endocannabinoids and beyond, Nat Rev Neurosci. 15 (2014) 757–764, https://doi.org/10.1038/nrn3811.

[7] F. Patricio, A.A. Morales-Andrade, A. Patricio-Martínez, I.D. Limón, Cannabidiol as a Therapeutic Target: Evidence of its Neuroprotective and Neuromodulatory Function in Parkinson's Disease, Front Pharmacol. 11 (2020), https://doi.org/10.3389/fphar.2020.595635.

[8] J. Peng, M. Fan, C. An, F. Ni, W. Huang, J. Luo, A narrative review of molecular mechanism and therapeutic effect of cannabidiol (CBD), Basic Clin Pharmacol Toxicol. (2022), https://doi.org/10.1111/BCPT.13710.

[9] A. Talwar, E. Estes, R. Aparasu, D.S. Reddy, Clinical efficacy and safety of cannabidiol for pediatric refractory epilepsy indications: A systematic review and meta-analysis, Exp Neurol. (2022), 114238, https://doi.org/10.1016/j.expneurol.2022.114238.

[10] O.S. Miller, E.J. Elder, K.J. Jones, B.E. Gidal, Analysis of cannabidiol (CBD) and THC in nonprescription consumer products: Implications for patients and practitioners, Epilepsy Behav. 127 (2022), 108514, https://doi.org/10.1016/J.YEBEH.2021.108514.

[11] R.M. Vitale, F.A. Iannotti, P. Amodeo, The (Poly)Pharmacology of Cannabidiol in Neurological and Neuropsychiatric Disorders: Molecular Mechanisms and Targets, Int. J. Mol. Sci. 22 (2021) 4876, https://doi.org/10.3390/ijms22094876.

[12] L.K. Peltner, L. Gluthmann, F. Börner, S. Pace, R.K. Hoffstetter, C. Kretzer, R. Bilancia, F. Pollastro, A. Koeberle, G. Appendino, A. Rossi, M.E. Newcomer, N. C. Gilbert, O. Werz, P.M. Jordan, Cannabidiol acts as molecular switch in innate immune cells to promote the biosynthesis of inflammation-resolving lipid mediators, Cell Chem Biol 30 (2023) 1–17, https://doi.org/10.1016/j.chembiol.2023.08.001.

[13] E.C. Rosenberg, S. Chamberland, M. Bazelot, E.R. Nebet, X. Wang, S. McKenzie, S. Jain, S. Greenhill, M. Wilson, N. Marley, A. Salah, S. Bailey, P.H. Patra, R. Rose, N. Chenouard, S.D. Sun, D. Jones, G. Buzsáki, O. Devinsky, G. Woodhall, H. E. Scharfman, B.J. Whalley, R.W. Tsien, Cannabidiol modulates excitatory-inhibitory ratio to counter hippocampal hyperactivity, Neuron 111 (2023) 1282–1300.e8, https://doi.org/10.1016/j.neuron.2023.01.018.

[14] T. Cordova, D. Ayalon, N. Lander, R. Mechoulam, I. Nir, M. Puder, H.R. Lindner, The ovulation blocking effect of cannabinoids: Structure-activity relationships, Psychoneuroendocrinology 5 (1980) 53–62, https://doi.org/10.1016/0306-4530(80)90009-8.

[15] A. Juknat, E. Kozela, N. Kaushansky, R. Mechoulam, Z. Vogel, Anti-inflammatory effects of the cannabidiol derivative dimethylheptyl-cannabidiol - Studies in BV-2 microglia and encephalitogenic T cells, J Basic Clin Physiol Pharmacol. 27 (2016) 289–296, https://doi.org/10.1515/jbcpp-2015-0071.

[16] R.L. Silva, G.T. Silveira, C.W. Wanderlei, N.T. Cecilio, A.G.M. Maganin, M. Franchin, L.M.M. Marques, N.P. Lopes, J.A. Crippa, F.S. Guimarães, J.C. F. Alves-Filho, F.Q. Cunha, T.M. Cunha, DMH-CBD, a cannabidiol analog with

reduced cytotoxicity, inhibits TNF production by targeting NF-kB activity dependent on A$_{2A}$ receptor, Toxicol Appl Pharmacol. 368 (2019) 63–71, https://doi.org/10.1016/j.taap.2019.02.011.

[17] S. Ben-Shabat, L.O. Hanuš, G. Katzavian, R. Gallily, New cannabidiol derivatives: Synthesis, binding to cannabinoid receptor, and evaluation of their antiinflammatory activity, J Med Chem. 49 (2006) 1113–1117, https://doi.org/10.1021/jm050709m.

[18] R. Gallily, T. Even-Chen, G. Katzavian, D. Lehmann, A. Dagan, R. Mechoulam, γ-Irradiation enhances apoptosis induced by cannabidiol, a non-psychotropic cannabinoid, in cultured HL-60 myeloblastic leukemia cells, Leuk Lymphoma. 44 (2003) 1767–1773, https://doi.org/10.1080/1042819031000103917.

[19] E. Fride, D. Ponde, A. Breuer, L. Hanuš, Peripheral, but not central effects of cannabidiol derivatives: Mediation by CB1 and unidentified receptors, Neuropharmacology 48 (2005) 1117–1129, https://doi.org/10.1016/j.neuropharm.2005.01.023.

[20] T. Bisogno, L. Hanuš, L. De Petrocellis, S. Tchilibon, D.E. Ponde, I. Brandi, A. S. Moriello, J.B. Davis, R. Mechoulam, V. Di Marzo, Molecular targets for cannabidiol and its synthetic analogues: Effect on vanilloid VR1 receptors and on the cellular uptake and enzymatic hydrolysis of anandamide, Br J Pharmacol. 134 (2001) 845–852, https://doi.org/10.1038/sj.bjp.0704327.

[21] L.O. Hanuš, S. Tchilibon, D.E. Ponde, A. Breuer, E. Fride, R. Mechoulam, Enantiomeric cannabidiol derivatives: Synthesis and binding to cannabinoid receptors, Org Biomol Chem. 3 (2005) 1116–1123, https://doi.org/10.1039/b416943c.

[22] M. Tham, O. Yilmaz, M. Alaverdashvili, M.E.M. Kelly, E.M. Denovan-Wright, R. B. Laprairie, Allosteric and orthosteric pharmacology of cannabidiol and cannabidiol-dimethylheptyl at the type 1 and type 2 cannabinoid receptors, Br J Pharmacol. 176 (2019) 1455–1469, https://doi.org/10.1111/BPH.14440.

[23] F. Gado, S. Meini, S. Bertini, M. Digiacomo, M. Macchia, C. Manera, Allosteric modulators targeting cannabinoid cb1 and cb2 receptors: implications for drug discovery, Future, Med Chem. 11 (2019) 2019–2037, https://doi.org/10.4155/fmc-2019-0005.

[24] P.K. Smith, R.I. Krohn, G.T. Hermanson, A.K. Mallia, F.H. Gartner, M. D. Provenzano, E.K. Fujimoto, N.M. Goeke, B.J. Olson, D.C. Klenk, Measurement of protein using bicinchoninic acid, Anal Biochem. 150 (1985) 76–85.

[25] A. Martella, H. Sijben, A.C. Rufer, U. Grether, J. Fingerle, C. Ullmer, T. Hartung, A. P. IJzerman, M. van der Stelt, L.H. Heitman, A Novel Selective Inverse Agonist of the CB$_2$ Receptor as a Radiolabeled Tool Compound for Kinetic Binding Studies, Mol Pharmacol. 92 (2017) 389–400. https://doi.org/10.1124/mol.117.108605.

[26] X. Li, H. Chang, J. Bouma, L.V. de Paus, P. Mukhopadhyay, J. Paloczi, M. Mustafa, C. van der Horst, S.S. Kumar, L. Wu, Y. Yu, R.J.B.H.N. van den Berg, A.P. A. Janssen, A. Lichtman, Z.-J. Liu, P. Pacher, M. van der Stelt, L.H. Heitman, T. Hua, Structural basis of selective cannabinoid CB2 receptor activation, Nat Commun. 14 (2023) 1–16, https://doi.org/10.1038/s41467-023-37112-9.

[27] M. Tonelli, E. Cichero, A.M. Mahmoud, A. Rabbito, B. Tasso, P. Fossa, A. Ligresti, Exploring the effectiveness of novel benzimidazoles as CB2 ligands: synthesis, biological evaluation, molecular docking studies and ADMET prediction, Medchemcomm. 9 (2018) 2045–2054, https://doi.org/10.1039/C8MD00461G.

[28] J. Bouma, M. Soethoudt, N. van Gils, L. Xia, M. van der Stelt, L.H. Heitman, Cellular Assay to Study β-Arrestin Recruitment by the Cannabinoid Receptors 1 and 2, in: M. Maccarrone (Ed.), Endocannabinoid Signaling. Methods in Molecular Biology, Humana, New York, NY, 2023, pp. 189–199, https://doi.org/10.1007/978-1-0716-2728-0_15.

[29] DiscoverX, User Manual PathHunter® Detection Kit, (n.d.). https://www.discoverx.com/DiscoveRx/media/ContentFiles/DataSheets/93-0001L.pdf (accessed September 8, 2021).

[30] Y.-C. Cheng, W.H. Prusoff, Relationship between the inhibition constant (K1) and the concentration of inhibitor which causes 50 per cent inhibition (I50) of an enzymatic reaction, Biochem Pharmacol. 22 (1973) 3099–3108, https://doi.org/10.1016/0006-2952(73)90196-2.

[31] N. Martinez Naya, J. Kelly, G. Corna, M. Golino, A. Abbate, S. Toldo, Molecular and Cellular Mechanisms of Action of Cannabidiol, Molecules 28 (2023), https://doi.org/10.3390/molecules28165980.

[32] A. Christopoulos, T. Kenakin, G protein-coupled receptor allosterism and complexing, Pharmacol Rev. 54 (2002) 323–374, https://doi.org/10.1124/pr.54.2.323.

[33] T.P. Kenakin, Biased signalling and allosteric machines: new vistas and challenges for drug discovery, Br J Pharmacol. 165 (2012) 1669, https://doi.org/10.1111/bph.2012.165.issue-6.

[34] J.R. Lane, L.T. May, R.G. Parton, P.M. Sexton, A. Christopoulos, A kinetic view of GPCR allostery and biased agonism, Nat Chem Biol. 13 (2017) 929–937, https://doi.org/10.1038/nchembio.2431.

[35] K. Leach, P.M. Sexton, A. Christopoulos, Quantification of allosteric interactions at G protein-coupled receptors using radioligand binding assays., Current Protocols in Pharmacology / Editorial Board, S.J, Enna (editor-in-Chief) [et Al.]. Chapter 1 (2011), https://doi.org/10.1002/0471141755.ph0122s52.

[36] P. Pandey, K.K. Roy, R.J. Doerksen, Negative allosteric modulators of cannabinoid receptor 2: protein modeling, binding site identification and molecular dynamics simulations in the presence of an orthosteric agonist, J Biomol Struct Dyn. 38 (2020) 32–47, https://doi.org/10.1080/07391102.2019.1567384.

[37] M. Rajasekaran, Characterization of allosteric modulators of CB2 receptors as novel therapeutics for inflammatory diseases, University of Arkansas for Medical Sciences, 2011. PhD thesis.

[38] V. Petrucci, A. Chicca, S. Glasmacher, J. Paloczi, Z. Cao, P. Pacher, J. Gertsch, Pepcan-12 (RVD-hemopressin) is a CB2 receptor positive allosteric modulator constitutively secreted by adrenals and in liver upon tissue damage, Sci Rep. 7 (2017) 1–14, https://doi.org/10.1038/s41598-017-09808-8.

[39] D. Guo, L.A. Peletier, L. Bridge, W. Keur, H. de Vries, A. Zweemer, L.H. Heitman, A. P. IJzerman, A two-state model for the kinetics of competitive radioligand binding, Br J Pharmacol. 175 (2018) 1719–1730. https://doi.org/10.1111/bph.14184.

[40] J. Gertsch, M. Leonti, S. Raduner, I. Racz, J.-Z. Chen, X.-Q. Xie, K-H. Altmann, M. Karsak, A. Zimmer, Beta-caryophyllene is a dietary cannabinoid, PNAS 105 (2008) 9099–9104, https://doi.org/10.1073/pnas.0803601105.

[41] A. Chicca, D. Caprioglio, A. Minassi, V. Petrucci, G. Appendino, O. Tagliatela-Scafati, J. Rg Gertsch, Functionalization of β-Caryophyllene Generates Novel Polypharmacology in the Endocannabinoid System, ACS Chem. Biol. 9 (2014) 30, https://doi.org/10.1021/cb500177c.

[42] G. Navarro, A. Gonzalez, A. Sánchez-Morales, N. Casajuana-Martin, M. Gómez-Ventura, A. Cordomí, F. Busqué, R. Alibés, L. Pardo, R. Franco, Design of Negative and Positive Allosteric Modulators of the Cannabinoid CB$_2$ Receptor Derived from the Natural Product Cannabidiol, J Med Chem. (2021), https://doi.org/10.1021/acs.jmedchem.1c00561.

[43] L.M. Slosky, M.G. Caron, L.S. Barak, Biased Allosteric Modulators: New Frontiers in GPCR Drug Discovery, Trends Pharmacol Sci. 42 (2021) 283–299, https://doi.org/10.1016/j.tips.2020.12.005.

[44] M.S. Ibsen, D.B. Finlay, M. Patel, J.A. Javitch, M. Glass, N.L. Grimsey, Cannabinoid CB1 and CB2 Receptor-Mediated Arrestin Translocation: Species, Subtype, and Agonist-Dependence, Front Pharmacol. 10 (2019), https://doi.org/10.3389/FPHAR.2019.00350.

[45] T. Kenakin, The quantitative characterization of functional allosteric effects, Curr Protoc Pharmacol. (2017) 9.22.1-9.22.10. https://doi.org/10.1002/cpph.18.

[46] A. Bock, M. Bermudez, F. Krebs, C. Matera, B. Chirinda, D. Sydow, C. Dallanoce, U. Holzgrabe, M. De Amici, M.J. Lohse, G. Wolber, K. Mohr, Ligand binding ensembles determine graded agonist efficacies at a G protein-coupled receptor, J. Biol. Chem. 291 (2016) 16375–16389, https://doi.org/10.1074/jbc.M116.735431.

[47] T.P. Kenakin, A pharmacology primer: techniques for more effective and strategic drug discovery, Fourth edition, Academic Press, 2014.

[48] A.C. Kruse, A.M. Ring, A. Manglik, J. Hu, K. Hu, K. Eitel, H. Hübner, E. Pardon, C. Valant, P.M. Sexton, A. Christopoulos, C.C. Felder, P. Gmeiner, J. Steyaert, W. I. Weis, K.C. Garcia, J. Wess, B.K. Kobilka, Activation and allosteric modulation of a muscarinic acetylcholine receptor, Nature 504 (2013) 101–106, https://doi.org/10.1038/nature12735.

[49] J. Yuan, C. Jiang, J. Wang, C.J. Chen, Y. Hao, G. Zhao, Z. Feng, X.Q. Xie, In Silico Prediction and Validation of CB2 Allosteric Binding Sites to Aid the Design of Allosteric Modulators, Molecules 27 (2022) 453, https://doi.org/10.3390/MOLECULES27020453.

[50] M. Congreve, C. Oswald, F.H. Marshall, Applying Structure-Based Drug Design Approaches to Allosteric Modulators of GPCRs, Trends Pharmacol Sci. 38 (2017) 837–847, https://doi.org/10.1016/j.tips.2017.05.010.